Available online at www.sciencedirect.com
SCIENCE DIRECT®
Acta Materialia 52 (2004) 4093–4099
Acta MATERIALIA
www.actamat-journals.com

Super-high strength of over 4000 MPa for Fe-based bulk glassy alloys in $[(Fe_{1-x}Co_x)_{0.75}B_{0.2}Si_{0.05}]_{96}Nb_4$ system

A. Inoue [a], B.L. Shen [a,*], C.T. Chang [b]

[a] *Institute for Materials Research, Tohoku University, Katahira 2-1-1, Aoba-ku, Sendai 980-8577, Japan*
[b] *Graduate School, Tohoku University, Sendai 980-8577, Japan*

Received 27 February 2004; received in revised form 11 May 2004; accepted 13 May 2004
Available online 8 June 2004

Abstract

New Fe-based bulk glassy alloys with diameters up to 5 mm were formed in $[(Fe_{1-x}Co_x)_{0.75}B_{0.2}Si_{0.05}]_{96}Nb_4$ system by the copper mold casting method. The substitution of Co for Fe causes an increase in the glass-forming ability (GFA). As the Co content increases, the liquidus temperature (T_l) decreases, resulting in an increase of reduced glass transition temperature (T_g/T_l) from 0.566 to 0.587. The bulk glassy alloys exhibit super-high fracture strength of 3900–4250 MPa, Young's modulus (E) of 190–210 GPa, elastic strain (ε_e) of 0.02, plastic strain (ε_p) of 0.0025 and Vickers hardness (H_v) of 1150–1220. The σ_f/E and $H_v/3E$ of these glassy alloys are 0.02, respectively, in agreement with the previous data for a number of bulk glassy alloys. The agreement indicates that these Fe-based bulk glassy alloys have an elastic–plastic deformation mode. The syntheses of high-strength Fe-based bulk glassy alloys with super-high fracture strength of over 4000 MPa and high glass-forming ability are encouraging for future development of Fe-based bulk glassy alloys as structural materials.

Keywords: Metallic glasses; Compression test; Hardness test; Slip markings; Mechanical properties

1. Introduction

Since bulk glassy alloys with high strength were synthesized in Mg- [1], Ln- [2] and Zr- [3,4] based alloy systems by various casting methods for several years between 1988 and 1990, great efforts have been devoted to the syntheses of bulk glassy alloys with high strength. For example, Zr-based bulk glassy alloys with fracture strength of about 1700 MPa in conjunction with high glass-forming ability have been used as practical materials such as sporting goods, connecting parts for optical fibers and casing for portable electro-magnetic instruments by taking advantages of high strength and large elastic strain [5–8]. It has subsequently been reported that high strength characteristics exceeding 2000 MPa are obtained in Cu- [9], Ni- [10] and Co–Fe- [11] based bulk glassy alloys. When we focus on Fe-based bulk glassy alloys, much attention has been paid to magnetic properties [12] and some Fe-based bulk glassy alloys have also been used as soft electro-magnetic cores for common mode choke coil and noise filter [13]. Mechanical properties of Fe-based bulk glassy alloys were also measured for alloy compositions of $Fe_{77}Ga_3P_{9.5}C_4B_4Si_{2.5}$ and $(Fe_{0.75}B_{0.15}Si_{0.1})_{96}Nb_4$ [14]. The yield strength and fracture strength were reported to be 2978–3160 and 3162–3250 MPa, respectively, for the $Fe_{77}Ga_3P_{9.5}C_4B_4Si_{2.5}$ and $(Fe_{0.75}B_{0.15}Si_{0.1})_{96}Nb_4$ bulk glassy alloys. Recently, Ponnambalam et al. [15] introduced a new class of Fe-based bulk metallic glasses as non-ferromagnetic amorphous steel alloys that were found to exhibit fracture strengths of 3000–4000 MPa. Very recently, we have found that much higher fracture strength exceeding 4000 MPa is obtained for Fe–Co–B–Si–Nb bulk glassy alloys. It is important to clarify the effect of the replacement of Fe by Co as well as the increase of B to Si concentration ratio with the aim of developing a new Fe-based bulk glassy alloy with higher strength and higher glass-forming ability. This paper

* Corresponding author. Tel.: +81-22-215-2113; fax: +81-22-215-2111.
E-mail address: shen@imr.tohoku.ac.jp (B.L. Shen).

1359-6454/$30.00 © 2004 Acta Materialia Inc. Published by Elsevier Ltd. All rights reserved.
doi:10.1016/j.actamat.2004.05.022

intends to present the compositional dependence of glass-forming ability and thermal stability for melt-spun $[(Fe_{1-x}Co_x)_{0.75}B_{0.2}Si_{0.05}]_{96}Nb_4$ glassy alloys as well as the formation and mechanical properties of the resulting Fe–Co-based bulk glassy alloys and to investigate the effectiveness of the replacement of Fe by Co.

2. Experimental procedure

Multi-component Fe-based alloy ingots with compositions of $[(Fe_{1-x}Co_x)_{0.75}B_{0.2}Si_{0.05}]_{96}Nb_4$ ($x = 0$–0.5) were prepared by arc melting the mixtures of pure Fe, Co and Nb metals and pure B and Si crystals in an argon atmosphere. The alloy compositions represent nominal atomic percentages. Bulk glassy alloy rods with diameters of 1–5 mm were produced by the ejection copper mold casting method. Glassy alloy ribbons with a cross section of 0.02×1.2 mm^2 were also produced by the melt spinning method. The glassy structure was identified by X-ray diffraction and the absence of micrometer scale crystalline phase was examined by optical microscopy. Thermal stability associated with glass transition temperature (T_g), crystallization temperature (T_x), and supercooled liquid region ($\Delta T_x = T_x - T_g$) was examined by differential scanning calorimetry (DSC) at a heating rate of 0.67 K/s. It is known that liquidus line (or primary crystal line) temperature (T_l) is the temperature of the crystalline phase precipitating from liquid. Consequently, the T_l of alloys was measured by cooling the molten alloy samples with a differential thermal analyzer (DTA). To reduce influence of undercooling, the DTA measurement was performed at a very low cooling rate of 0.033 K/s. Mechanical properties of Young's modulus, compressive fracture strength, elastic strain and plastic strain were measured with an Instron testing machine. The gauge dimension was 1.5–2.0 mm in diameter and 3–4 mm in length and the strain rate was 6.0×10^{-4} s^{-1} for the 3 mm sample and 5.0×10^{-4} s^{-1} for the 4 mm sample. Vickers hardness was measured with a Vickers hardness tester under a load of 1.96 N. Deformation and fracture behaviors were examined by scanning electron microscopy (SEM).

3. Results

Fig. 1 shows DSC curves of the $[(Fe_{1-x}Co_x)_{0.75}B_{0.2}Si_{0.05}]_{96}Nb_4$ glassy alloys produced by melt spinning. All the alloys exhibit glass transition, followed by a supercooled liquid region and then crystallization. Although T_g and T_x decrease gradually from 835 to 820 and 880 to 870 K, respectively, with an increase of Co content, ΔT_x keeps a nearly constant value of 50 K. It is also seen that these glassy alloys have a ferromagnetic state and the transition from ferromagnetic to paramagnetic state occurs at 598–692 K as marked with Curie temperature (T_c). The T_c increases with an increase of Co content because of the strong exchange coupling between Fe and Co elements. In addition, by substituting Co for Fe, the difference between two exothermic peaks becomes large. When the Co content is equal to Fe content, the crystallization of the Fe-based glassy alloys occurs through a mostly single exothermic reaction. We have also examined the composition dependence of the reduced glass transition temperature (T_g/T_l) for the $[(Fe_{1-x}Co_x)_{0.75}B_{0.2}Si_{0.05}]_{96}Nb_4$ glassy alloys. As shown in Fig. 2, the T_l decreases from 1475 to 1395 K with an increase of Co content, resulting in the increase of T_g/T_l from 0.566 to 0.587, indicating that higher glass-forming ability may be obtained in the Co-containing alloy system.

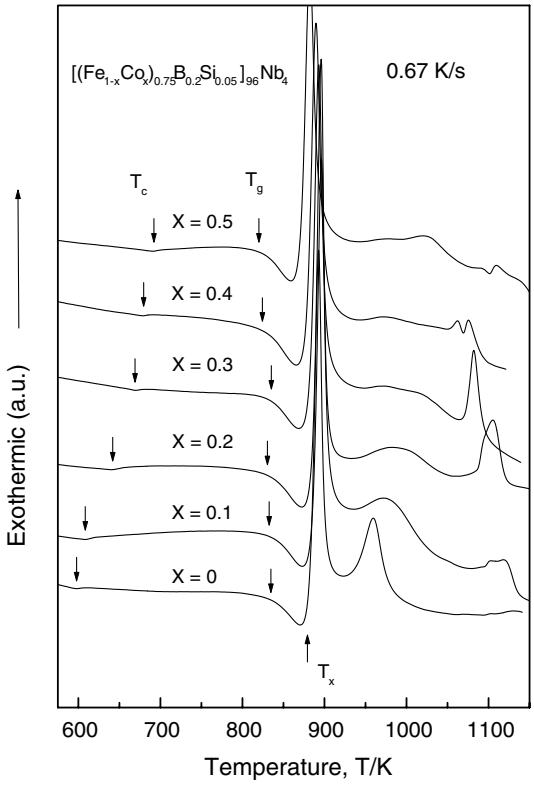

Fig. 1. DSC curves of melt-spun $[(Fe_{1-x}Co_x)_{0.75}B_{0.2}Si_{0.05}]_{96}Nb_4$ ($x = 0$, 0.1, 0.2, 0.3, 0.4 and 0.5) glassy alloy ribbons.

We tried to form cylindrical glassy alloy rods with different diameters up to 6 mm by the copper mold casting method for this alloy system. The glassy alloy rods were produced at all alloy compositions in this system. The critical diameter for formation of a glassy single phase was 1.5 mm at $x = 0$, 2 mm at $x = 0.1$, 2.5 mm at $x = 0.2$, 3.5 mm at $x = 0.3$, 4 mm at $x = 0.4$ and 5 mm at $x = 0.5$. Fig. 3 shows outer surface and morphology of the cast glassy alloy rods with diameters of 2.5–5 mm. The outer surface is very smooth and neither concave nor ruggedness due to a crystalline

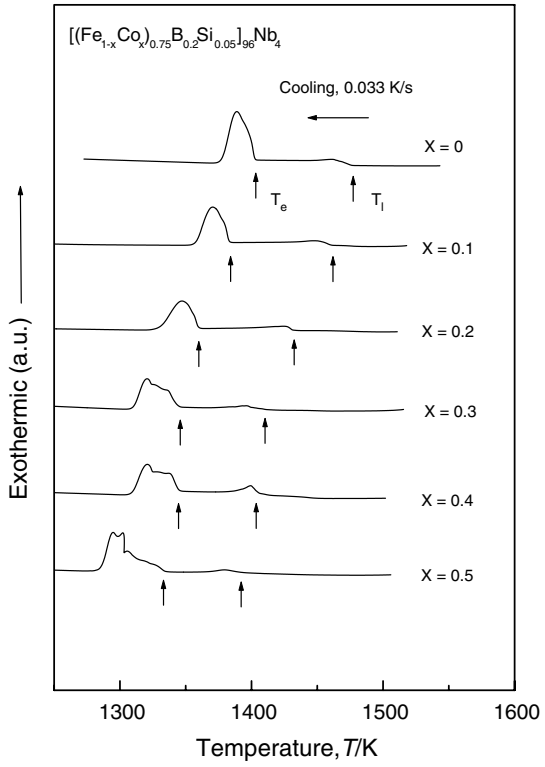

Fig. 2. DTA curves of $[(Fe_{1-x}Co_x)_{0.75}B_{0.2}Si_{0.05}]_{96}Nb_4$ ($x = 0$, 0.1, 0.2, 0.3, 0.4 and 0.5) alloys.

Fig. 3. Outer surface and morphology of the cast glassy alloy rods with critical diameters of 2.5–5 mm.

phase is seen for all the rod samples. Fig. 4 shows X-ray diffraction patterns of those cast alloy rods. Only broad peaks without crystalline peak can be seen for all these bulk samples, indicating the formation of a glassy phase in the diameter range up to 5 mm. We have also confirmed the formation of glassy alloy rods without micrometer scale crystalline phase by optical microscopy. It is noticed that the minimum diameter of 2 mm for glass formation of the Fe–Co-based alloys is larger than

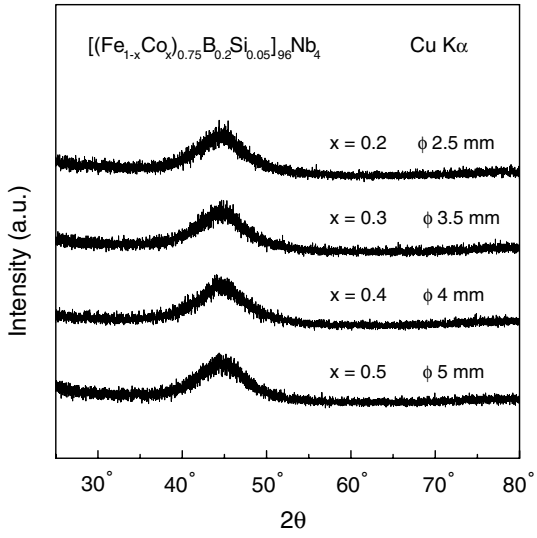

Fig. 4. X-ray diffraction patterns of cast $[(Fe_{1-x}Co_x)_{0.75}B_{0.2}Si_{0.05}]_{96}Nb_4$ ($x = 0.2$, 0.3, 0.4 and 0.5) rods with diameters of 2.5, 3.5, 4 and 5 mm, respectively.

the previous reported maximum value (1.5 mm) for Fe–B–Si–Nb alloys [16]. As an example, Fig. 5 shows DSC curves of the cast glassy $[(Fe_{0.8}Co_{0.2})_{0.75}B_{0.2}Si_{0.05}]_{96}Nb_4$ alloy rods with diameters up to 2.5 mm. The data of the melt-spun glassy alloy ribbon are also shown for comparison. It is seen that the bulk alloys exhibit distinct

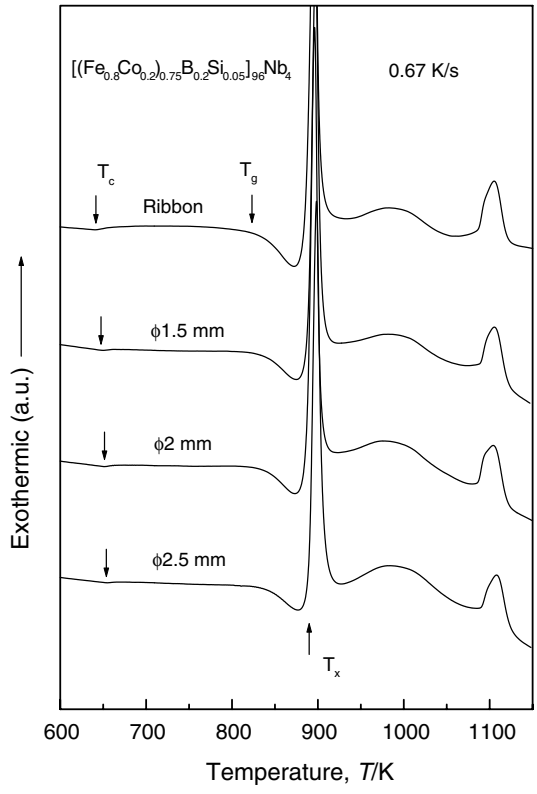

Fig. 5. DSC curves of bulk glassy $[(Fe_{0.8}Co_{0.2})_{0.75}B_{0.2}Si_{0.05}]_{96}Nb_4$ alloy rods with diameters of 1.5, 2 and 2.5 mm. The data of the melt-spun glassy alloy ribbon are also shown for comparison.

glass transition at 830 K, followed by a large supercooled liquid region of 50 K. No appreciable difference in T_g, T_x, ΔT_x and crystallization process is recognized between the melt-spun ribbon and rod samples, though Curie temperature (T_c) increases with an increase of diameter. This result indicates clearly the formation of the Fe-based glassy alloy rods with diameters up to 2.5 mm. The increase of T_c is interpreted to result from the progress of structural relaxation as the diameter of the glassy alloy rod increases [17].

By using these Fe-based glassy alloy rods of 2 mm in diameter, we measured mechanical properties by compressive test. The alloys exhibit the similar features, i.e., elastic deformation up to a strain of about 0.02, followed by small plastic strain of about 0.0025 and then final fracture. The mechanical properties of the $(Fe_{0.75}B_{0.2}Si_{0.05})_{96}Nb_4$ glassy alloy with a diameter of 1.5 mm were also used for comparison. Fig. 6 shows the compressive true stress–strain curve of the $[(Fe_{0.8}Co_{0.2})_{0.75}B_{0.2}Si_{0.05}]_{96}Nb_4$ glassy alloy rod with a diameter of 2 mm. The Young's modulus (E), yield strength (σ_y) defined by the deviation from the linear relation, fracture strength (σ_f), elastic strain (ε_e) and fracture strain (ε_f) are 203, 4050, 4170 MPa, 0.02 and 0.0225, respectively. In addition, Vickers hardness number was measured as 1225. It is noticed that this Fe-based bulk glassy alloy rod exhibits very high strength of 4170 MPa combined with plastic strain of about 0.0025. Fig. 7 shows SEM image revealing deformation behavior of the alloy rod with the σ_f of 4170 MPa subjected to the strain of 0.0215 but unloaded before fracture. A localized main shear band can be observed on the surface of the rod as shown in Fig. 7, and its angle with stress axis is measured to be 44°, which is in agreement with the other results [18]. Fig. 8 shows the fracture surface morphology of the Fe-based bulk glassy alloy rod. The fracture surface consists of a number of small fracture zones and their zone planes appear to be

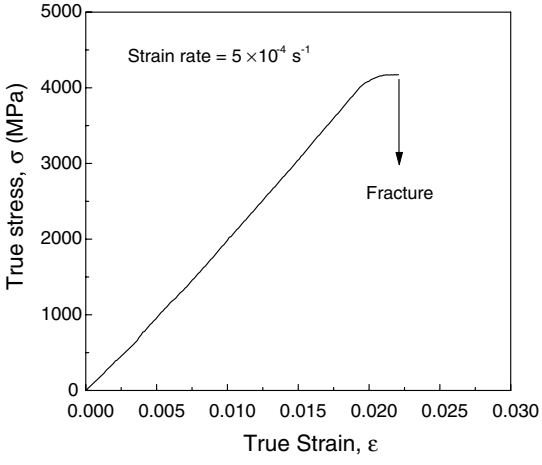

Fig. 6. Compressive true stress–strain curve of a bulk glassy $[(Fe_{0.8}Co_{0.2})_{0.75}B_{0.2}Si_{0.05}]_{96}Nb_4$ alloy rod with a diameter of 2 mm.

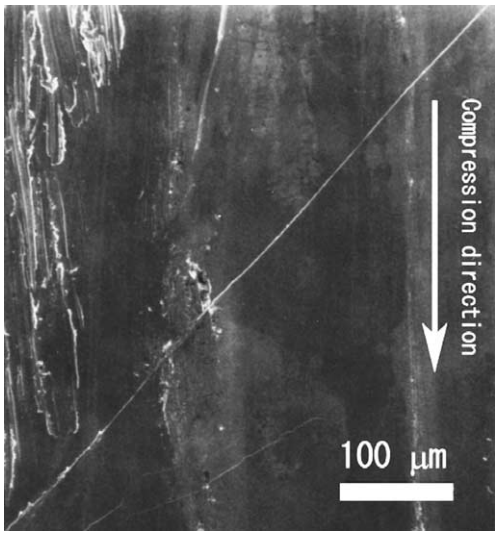

Fig. 7. Scanning electron micrograph (SEM) image of outer lateral surface of the bulk glassy $[(Fe_{0.8}Co_{0.2})_{0.75}B_{0.2}Si_{0.05}]_{96}Nb_4$ alloy rod subjected to the strain of 0.0215 but unloaded before fracture.

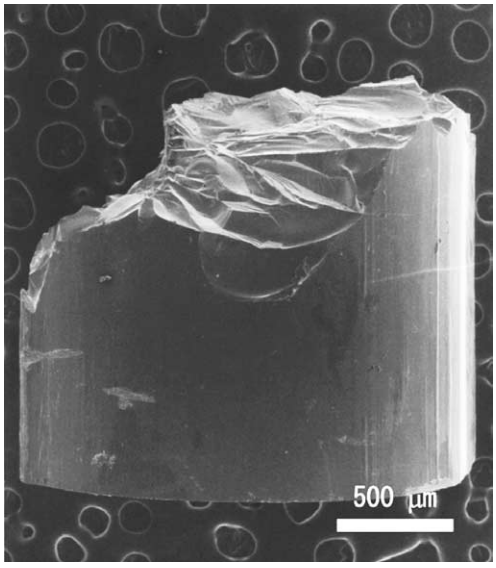

Fig. 8. Fracture surface morphology of the cast $[(Fe_{0.8}Co_{0.2})_{0.75}B_{0.2}Si_{0.05}]_{96}Nb_4$ glassy alloy rod subjected to compressive deformation test.

declined by about 55–90° to the direction of applied load. The fracture behavior is different from the previous results [5,9,10] for Zr-, Cu- and Ni-based bulk glassy alloys where the fracture occurs only along the maximum shear plane which is declined by about 45° to the direction of applied load, but nearly the same with the previous results of Fe-based bulk glassy alloys [14]. The nearly simultaneous generation of a number of small fracture zones is presumably due to easy initiation of fracture at many sites. The easy initiation may result from the mechanism in which the initiation of crack occurs at a very high stress level exceeding 4000 MPa and the shock

wave caused by its initiation induces the generation of cracks at different sites because of high fracture stress level due to strong bonding forces among the constituent elements. The fracture mechanism is also supported from the enlarged micrograph of the fracture surface revealing very fine shell pattern which appears to generate the propagation of the crack, as shown in Fig. 9.

We further examined the degree of brittleness of the Fe-based bulk glassy alloy rods by observing the generation of slip marking or crack around the indentation produced by a Vickers hardness indenter with different applied loads of 4.9 and 9.8 N. Fig. 10 shows the slip markings around the Vickers hardness indentation obtained with a rather high load of 9.8 N for the $[(Fe_{0.8}Co_{0.2})_{0.75}B_{0.2}Si_{0.05}]_{96}Nb_4$ glassy alloy rod. A number of slip markings are seen in the vicinity of the indentation. The generation of a number of slip markings as well as the absence of appreciable crack also indicates that the Fe-based bulk glassy alloys are ductile enough to exhibit the above-described elastic–plastic deformation mode.

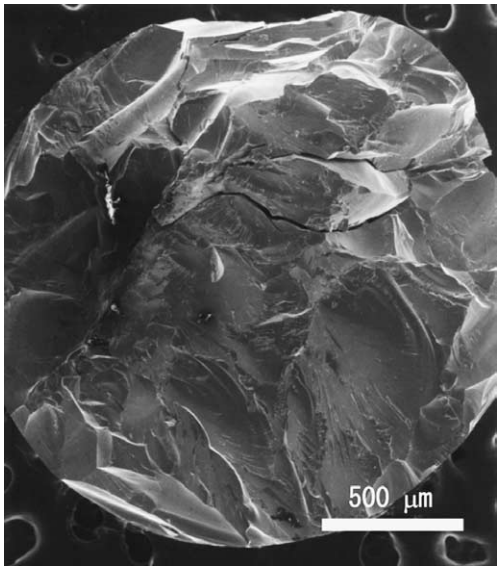

Fig. 9. Enlarged fracture surface of the cast $[(Fe_{0.8}Co_{0.2})_{0.75}B_{0.2}Si_{0.05}]_{96}Nb_4$ glassy alloy rod subjected to compressive deformation test.

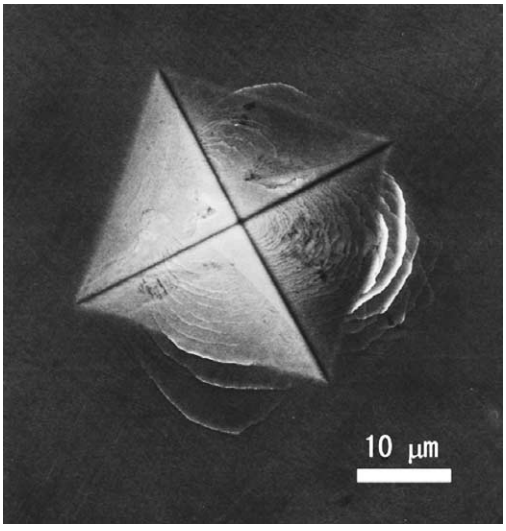

Fig. 10. Slip markings of a bulk glassy $[(Fe_{0.8}Co_{0.2})_{0.75}B_{0.2}Si_{0.05}]_{96}Nb_4$ alloy rod generated by indentation of a Vickers indenter with a load of 9.8 N.

4. Discussion

Table 1 summarizes maximum diameter, mechanical properties and thermal stability of the $[(Fe_{1-x}Co_x)_{0.75}B_{0.2}Si_{0.05}]_{96}Nb_4$ ($x = 0$, 0.1, 0.2, 0.3, 0.4 and 0.5) bulk glassy alloy rods. The values of σ_f/E, H_v/σ_f and $H_v/3E$ are about 0.02, 3.0 and 0.02, respectively. Considering that a number of amorphous and bulk glassy alloys reported up to date have nearly fixed values of about 0.02 for σ_f/E, 3.0 for H_v/σ_f and 0.02 for $H_v/3E$ [3,17], it is concluded that the present Fe-based bulk glassy alloys have the same ratios in their properties. The agreement also indicates that the Fe-based bulk glassy alloys have an elastic–plastic deformation mode without appreciable work hardening.

Fig. 11 summarizes the relation between σ_f and E of the Fe–B–Si–Nb and Fe–Co–B–Si–Nb glassy alloy rods together with the previous data of the other bulk glassy alloys and some typical crystalline materials [5–11]. The σ_f and E values of the present Fe-based alloys appear to lie in the same relation perfectly. There is a clear tendency for fracture strength to increase with increasing Young's modulus, but the slope of the linear relation corresponding to elastic elongation is significantly different between the bulk glassy and crystalline alloys and the elastic elongation of the glassy alloys is about three times larger than those for the crystalline alloys. The glassy alloys also exhibit high strength which is about three times higher than those for crystalline alloys, when the comparison is made at the same Young's modulus level. It is concluded that the new Fe–Co–B–Si–Nb glassy alloys have the highest strength for all Fe-based metallic bulk materials reported to date. These high values are interpreted to result from strong bonding nature among the constituent elements as is expected from the mixing enthalpies with large negative values. The enthalpy of mixing is −9 kJ/mol for the Co–B pair, −21 kJ/mol for the Co–Si pair, −25 kJ/mol for the Co–Nb pair, −11 kJ/mol for Fe–B pair, −18 kJ/mol for Fe–Si pair, −16 kJ/mol for Fe–Nb pair and −39 kJ/mol for B–Nb pair [19]. It can be seen that the mixing enthalpies with negative values of the atomic pairs between Co and Si or Nb are larger than those of the atomic pairs between Fe and Si or Nb, respectively, and the mixing enthalpy with negative values of the B–Nb atomic pair is

Table 1
Maximum diameters, thermal stability and mechanical properties of cast $[(Fe_{1-x}Co_x)_{0.75}B_{0.2}Si_{0.05}]_{96}Nb_4$ ($x = 0$, 0.1, 0.2, 0.3, 0.4 and 0.5) glassy alloy rods

Alloy	Thermal stability				Diameter	Mechanical properties						
	T_e (K)	T_g (K)	ΔT_x (K)	T_g/T_l	ϕ (mm)	H_v	E (GPa)	σ_y (MPa)	σ_f (MPa)	σ_f/E	H_v/σ_f	$H_v/3E$
$(Fe_{0.75}B_{0.2}Si_{0.05})_{96}Nb_4$	598	835	45	0.566	1.5	1070	180	3160	3400	0.019	3.1	0.02
$[(Fe_{0.9}Co_{0.1})_{0.75}B_{0.2}Si_{0.05}]_{96}Nb_4$	610	832	45	0.570	2	1150	190	3820	3900	0.021	3.0	0.02
$[(Fe_{0.8}Co_{0.2})_{0.75}B_{0.2}Si_{0.05}]_{96}Nb_4$	642	830	50	0.580	2.5	1225	205	4050	4170	0.020	2.9	0.02
$[(Fe_{0.7}Co_{0.3})_{0.75}B_{0.2}Si_{0.05}]_{96}Nb_4$	668	828	50	0.586	3.5	1245	210	4100	4200	0.020	3.0	0.02
$[(Fe_{0.6}Co_{0.4})_{0.75}B_{0.2}Si_{0.05}]_{96}Nb_4$	678	825	50	0.586	4	1250	210	4100	4250	0.020	2.9	0.02
$[(Fe_{0.5}Co_{0.5})_{0.75}B_{0.2}Si_{0.05}]_{96}Nb_4$	692	820	50	0.587	5	1220	210	4070	4210	0.020	2.9	0.019

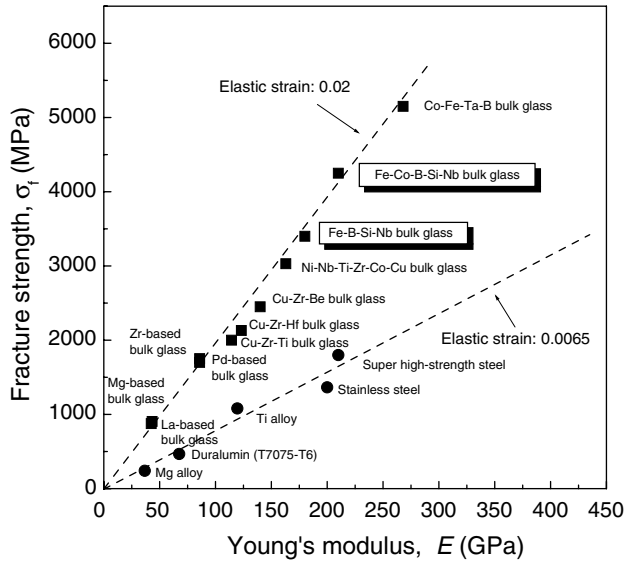

Fig. 11. Relation between compressive fracture strength (σ_f) and Young's modulus (E) for cast $(Fe_{0.75}B_{0.2}Si_{0.05})_{96}Nb_4$ and $[(Fe_{0.8}Co_{0.2})_{0.75}B_{0.2}Si_{0.05}]_{96}Nb_4$ glassy alloy rods. The present data are marked with open rectangles. The data of other bulk glassy and crystalline alloys are also shown for comparison.

as large as 39 kJ/mol. Therefore, it can be considered that the high glass-forming ability and super-high fracture strength of the present bulk glassy alloy system are resulted from the addition of Co as well as the increase of B. The atomic size difference between Co and B atoms is also significant as the radius is 0.125 nm for Co atom and 0.09 nm for the B atom [20]. It has previously been reported for Fe–Nb–B glassy alloys that the satisfaction of the three component rules, i.e., (1) multicomponent, (2) significant atomic size mismatches, and (3) negative heats of mixing, results in the formation of a unique network-like structure in which trigonal prisms consisting of Fe and B are connected with each other in an edge- and plane-shared configuration modes through glue atoms of Nb [21,22]. Furthermore, Poon et al. [23] have pointed out that the large (L) and small (S) atoms may form a strong L–S percolating network or reinforced 'backbone' in the amorphous structure, and presumably, the backbone structure can enhance the stability of the undercooled melt, which further suppresses crystallization. As the Co content increases, the crystallization of the Fe-based glassy alloys occurs through a mostly single exothermic reaction accompanying the increase of T_g/T_l. It can be also seen in Fig. 2 that the temperature interval between the eutectic temperature (T_e) and T_l decreases with increasing Co content, implying that the composition of the alloy with high Co content is close to that of eutectic alloy. These synergism effects enable us to prepare successfully bulk glassy alloy rods with large diameters up to 5 mm. The elastic strain of 0.02 at room temperature agrees well with the value (0.02) derived from the slope of linear

relation between strength and Young's modulus shown in Fig. 11, implying that the present high-strength glassy alloy also keeps an ideal elastic–plastic deformation mode [17] without strain-hardening ability. In any event, the agreement of the features in mechanical properties between the present Fe-based bulk glassy alloys and the other non-ferrous bulk glassy alloys is interpreted to result from the rather good deformability of the Fe-based alloys. This is consistent with the result in which a number of slip markings in the absence of appreciable crack are observed around the indentation obtained by a Vickers hardness indenter with a rather high load of 9.8 N.

5. Summary

We examined glass-forming ability, thermal stability and mechanical properties of Fe-based $[(Fe_{1-x}Co_x)_{0.75}B_{0.2}Si_{0.05}]_{96}Nb_4$ ($x = 0$–0.5) glassy alloys in melt-spun and cast states. The results obtained are summarized as follows:

1. All the alloys examined in the present study consist of a glassy phase in as-spun state. The glassy alloys exhibit distinct glass transition, followed by a supercooled liquid region and then crystallization. The supercooled liquid region and reduced glass transition temperature show maximum values of 50 K and 0.59, respectively.
2. Bulk glassy alloy rods with diameters larger than 2 mm were formed at all alloy compositions by the copper mold casting method. In particular, the bulk glassy alloy rods with large diameters up to 5 mm were formed for the $[(Fe_{0.5}Co_{0.5})_{0.75}B_{0.2}Si_{0.05}]_{96}Nb_4$ alloy with the largest ΔT_x and the highest T_g/T_l value. No appreciable difference in T_g, T_x and ΔT_x with rod diameter is recognized for all the alloys.
3. The $E, \sigma_y, \sigma_f, \varepsilon_e$ and ε_f of the present bulk glassy alloy rods are 190–215 GPa, 3820–4100, 3900–4250 MPa, 0.02 and 0.0225, respectively. It is noticed that the $[(Fe_{0.8}Co_{0.2})_{0.75}B_{0.2}Si_{0.05}]_{96}Nb_4$ glassy alloy exhibits super-high σ_f of over 4000 MPa in conjunction with distinct plastic strain of 0.0025.
4. The σ_f/E and $H_v/3E$ for the Fe-based bulk glassy alloys are 0.02, respectively, in agreement with the general tendency for bulk glassy alloys reported previously. The Fe-based bulk glassy alloys obey the elastic–plastic deformation behavior without strain hardening.
5. The alloys have the same linear relation between σ_f and E as that for the previously reported bulk glassy alloys. The super-high σ_f is concluded to result from the strong bonding forces among the constituent elements. The super-high strength combined with distinct plastic strain is promising for future development as a new type of structural or magnetic material.

References

[1] Inoue A, Ohtera K, Kita K, Masumoto T. Jpn J Appl Phys 1988;27:L2248.
[2] Inoue A, Zhang T, Masumoto T. Mater Trans JIM 1990;31:425.
[3] Inoue A, Zhang T, Masumoto T. Mater Trans JIM 1990;31:177.
[4] Peker A, Johnson WL. Appl Phys Lett 1993;63:2342.
[5] Inoue A, Zhang T. Mater Trans JIM 1995;36:1184.
[6] Inoue A. Acta Mater 2000;48:279.
[7] Kakiuchi A, Inoue A, Onuki M, Takano Y, Yamaguchi T. Mater Trans 2001;42:678.
[8] Ishida M, Takeda H, Yamaguchi T, Kita K. Mater Jpn 2003;42:585.
[9] Inoue A, Zhang W, Zhang T, Kurosaka K. Acta Mater 2001;49:2645.
[10] Zhang T, Inoue A. Mater Trans 2002;43:708.
[11] Inoue A, Shen BL, Koshiba H, Kato H, Yavari AR. Nat Mater 2003;2:661.
[12] Inoue A, Takeuchi A, Shen BL. Mater Trans 2002;42:970.
[13] Alps Electrical Corp. Ltd. Catalogue; 2002.
[14] Inoue A, Shen BL, Yavari AR, Greer AL. J Mater Res 2003;18:1487.
[15] Ponnambalam V, Poon SJ, Shiflet GJ, Keppens VM, Taylor R, Petculescu G. Appl Phys Lett 2003;83:1131.
[16] Inoue A, Shen BL. Mater Trans 2002;43:766.
[17] Chen HS. Rep Prog Phys 1980;43:353.
[18] Zhang ZF, Eckert J, Schultz L. Acta Mater 2003;51:1167.
[19] De Boer FR, Boom R, Mattens WCM, Miedema AR, Niessen AK. In: De Boer FR, Pettifor DG, editors. Cohesion in metals. Amsterdam: The North-Holland Physics Publishing; 1989. p. 217.
[20] Metals Databook, Tokyo: The Japan Institute of Metals, Maruzen; 1983. p. 8.
[21] Imafuku M, Sato S, Koshiba H, Matsubara E, Inoue A. Scr Mater 2001;44:2369.
[22] Imafuku M, Li C, Matsushita M, Inoue A. Jpn J Appl Phys 2002;41:219.
[23] Poon SJ, Shiflet GJ, Guo FQ, Ponnambalam V. J Non-Cryst Solids 2003;317:1.